

Isotope effects in lithium hydride and lithium deuteride crystals by molecular dynamics simulations

Hichem Dammak, Ekaterina Antoshchenkova, Marc Hayoun, Fabio Finocchi

► **To cite this version:**

Hichem Dammak, Ekaterina Antoshchenkova, Marc Hayoun, Fabio Finocchi. Isotope effects in lithium hydride and lithium deuteride crystals by molecular dynamics simulations. *Journal of Physics: Condensed Matter*, IOP Publishing, 2012, 24, pp.435402. 10.1088/0953-8984/24/43/435402 . hal-01932743

HAL Id: hal-01932743

<https://hal-centralesupelec.archives-ouvertes.fr/hal-01932743>

Submitted on 23 Nov 2018

HAL is a multi-disciplinary open access archive for the deposit and dissemination of scientific research documents, whether they are published or not. The documents may come from teaching and research institutions in France or abroad, or from public or private research centers.

L'archive ouverte pluridisciplinaire **HAL**, est destinée au dépôt et à la diffusion de documents scientifiques de niveau recherche, publiés ou non, émanant des établissements d'enseignement et de recherche français ou étrangers, des laboratoires publics ou privés.

Isotope effects in lithium hydride and lithium deuteride crystals by molecular dynamics simulations

‡

Hichem Dammak^{1,2}, Ekaterina Antoshchenkova¹, Marc Hayoun², Fabio Finocchi³

¹ Laboratoire Structures, Propriétés et Modélisation des Solides, CNRS UMR 8580, Ecole Centrale Paris, F-92295 Châtenay-Malabry, France

² Laboratoire des Solides Irradiés, Ecole Polytechnique, CEA-DSM, CNRS, F-91128 Palaiseau, France

³ Institut des Nano-Sciences de Paris, UPMC - Paris 6, UMR CNRS 7588, 4 place Jussieu, F-75251 Paris Cedex 5, France

E-mail: fabio.finocchi@upmc.fr

Abstract. Molecular dynamics (MD) simulations have been carried out to study isotope effects in lithium hydride and lithium deuteride crystals. Quantum effects on nuclear motion have been included through a quantum thermal bath (QTB). The interatomic forces were described either within the density-functional theory (DFT) in the generalized gradient approximation (GGA) or by the phenomenological approach using the shell model. For both models, the isotopic shift in the lattice parameter can be successfully predicted by QTB-MD simulations. The slope of the experimental isotopic shift in pressure is satisfactorily reproduced by QTB-MD within DFT-GGA, in contrast to both density-functional perturbation theory and QTB-MD with the shell model. We have analyzed the reasons of these discrepancies through the vibrational densities of states and the isotopic shifts in bulk modulus. The results illustrate the importance of anharmonic contributions to vibrations and to the isotopic pressure shift between LiH and LiD.

PACS numbers: 05.10.-a, 88.30.rd, 65.40.De, 67.63-r

1. Introduction

A considerable amount of experimental data and theoretical studies evidence that isotope substitution influences thermal, elastic and dynamical properties of crystals [1]. Isotope effects are especially pronounced whenever the reduced mass changes considerably. This happens in passing from LiH to LiD, two materials that have recently attracted much attention, as they are used in nuclear fusion [2] and are involved in hydrogen-based energy production [3].

From the theoretical point of view, ${}^7\text{LiH}$ and ${}^7\text{LiD}$ are relevant test cases for any method that includes the description of quantum effects [4]. In general, the crystal with lighter isotopes has larger lattice parameters. This purely quantum effect is due to the dependence of phonon frequencies on atomic masses and on anharmonic interactions. Isotope effects are important below Debye temperature, θ_D , and progressively weaken at higher temperatures.

Isotopic shift in the lattice parameter and in the equation of state of many crystals can be treated through the quasi harmonic approximation (QHA) [5]. However, this approach is not well suited for disordered systems, such as liquids, amorphous solids or crystals with defects. Moreover, many important dynamical phenomena, such as diffusion or density fluctuations, are outside the range of applicability of QHA.

Another technique that gives full access to statistical properties of materials, independently of their phase, is molecular dynamics (MD). However, in most cases, nuclei are treated as classical particles, and statistical averages are derived from classical partition functions. As quantum effects are missed, standard MD is suited at temperatures beyond θ_D . Nevertheless, some authors used standard MD to describe isotope effects in lithium hydrides, at the expense of introducing two distinct empirical interatomic potentials, one fitted for ${}^7\text{LiH}$ and the other for ${}^7\text{LiD}$ [6]. This procedure is questionable from the theoretical point of view, because isotope effects are primarily of statistical nature and are not a consequence of changes of interatomic interactions. Moreover, these potentials are not necessarily transferable to complex lithium hydride phases and might fail to describe isotope effects in a wide temperature range.

Quantum effects can be included in MD simulation through the well-known path-integral formalism of Feynmann [7]. This approach provides averages of physical quantities by taking into account the exact quantum statistical distributions. Unfortunately, it is very time consuming, which limits applications to complex or large systems. Recent alternatives consist in coupling the system to a quantum thermal bath (QTB) [8] or to a colored-noise thermostat [9]. Both approaches were designed to describe quantum nuclear dynamics and save at least two orders of magnitude of computer time with respect to path-integral MD technique [10, 11].

In this work, we combine QTB-MD with first-principles description of the potential energy surfaces, within the density functional theory (DFT). On one side, QTB-MD accounts for the quantum nature of the light H, D and ${}^7\text{Li}$ elements; on the other side, DFT provides a full description of the Li-H bond, in a large range of applied pressures.

We also present QTB-MD simulations based on an empirical interatomic potential [6]. The structure of the paper is as follows. The implementation of the QTB in the ABINIT code and the computational details are presented in section II. Section III reports the results of MD simulations for the isotope effects on the lattice parameter, on phonons and on the equation of state.

2. Computational Details

We employed the generalized gradient approximation (GGA) for describing the exchange-correlation energy, in the PBE form [12]. Previous numerical studies on LiH and LiD within the DFT employed pseudopotentials in order to describe the interaction between core ($1s$) electrons of Li and valence electrons from both Li and H. However, it appears that some structural and dynamical properties are sensitive to the relaxation of the Li core electrons [13]; therefore, we generated a norm-conserving pseudopotential for Li, within the Troullier-Martins scheme [14], by including the ($1s$) electrons in the valence. The reference atomic configuration was $(1s)^2(2s)^0(2p)^0$. $r_s = 1.45 a_0$ and $r_p = r_d = 1.3 a_0$ cutoff radii were adopted for the s , p and d components, respectively. The H pseudopotential has been generated in the Troullier-Martins scheme, with standard parameters [15]. Our calculations are thus all-electron, although Kohn-Sham orbitals were pseudized in the space region around the nuclei. Within this choice, static calculations, including no quantum effect, yielded converged lattice parameters for LiH already at 70 Ryd energy cutoff for the plane-waves basis set.

As a starting point, we computed the equilibrium lattice parameter, a_0 , the bulk modulus, B_0 , and its pressure derivative, B'_0 , within the static approximation, that is, neglecting any quantum motion. These quantities are given in table 1 and agree well with previous calculations [16, 17].

Table 1. Results of static calculations without taking into account the zero-point motion for LiH: lattice parameter a_0 , bulk modulus B_0 and pressure derivative B'_0 of bulk modulus. All calculations adopted the GGA for the exchange-correlation energy functional. We also specify the type of equation of state (EOS) used for fitting the numerical data.

| EOS | present Vinet [21] | Ref. [33] <i>not specified</i> | Ref. [17] Murnaghan [20] | Ref. [16] Birch [35] |
|-------------|-----------------------|-----------------------------------|-----------------------------|-------------------------|
| a_0 (Å) | 4.028 | 4.025 | 4.008 | 4.011 |
| B_0 (GPa) | 36.3 | 36.2 | 36.5 | 36.1 |
| B'_0 | 3.32 | | 3.63 | |

We implemented the Quantum Thermal Bath (QTB) in the parallel version of the ABINIT code [18, 19]. We started from ABINIT 6.0.4 and included the QTB by modifying subroutine moldyn. The reversible algorithm by Martyna and coworkers [22] was used to integrate the equations of motion. This algorithm allows to simulate either

the canonical (NVT) or the isobaric-isothermal (NPT) ensembles. In both cases, the classical thermostat of the original algorithm was replaced by the QTB [8]. The ABINIT code was very slightly modified, as the original atomic forces that are derived from the electronic structure are unchanged. Two additional contributions to atomic forces have been included: a dissipative force with an effective frictional coefficient and a Gaussian random force having the power spectral density given by the quantum fluctuation-dissipation theorem, thus different from a white noise as in classical Langevin dynamics. Before each run, random forces were generated according to the method described in Ref. [8] and by using a high-frequency cutoff ($\omega_{max} = 100$ THz, above the highest frequency of the physical LiH system), in order to avoid artifacts due to divergence of the energy spectral density at high frequencies [23]. Random forces were stored in a file that is read at each time step along the simulation.

In the equations of motion, the effective frictional coefficient was set at $\gamma = 10^{-4}$ au $^{-1}$, that is $\gamma = 0.414 \times 10^{13}$ s $^{-1}$. This value is smaller than the full width at half maximum of the simulated infrared absorption peak within the GGA. The mass of the barostat was fixed at $5 \times 10^6 m a_0^2$, where m is the electron mass and a_0 the Bohr radius. DFT simulations were performed for samples consisting of 64 atoms, in a cubic cell. Starting from the face-centered cubic structure, the system was equilibrated for several ps, for different temperatures ranging from 10K to 300K. Afterwards, statistics on the lattice constant in the (NPT) ensemble was taken for about 10 ps. We also calculated the pressure for ${}^7\text{LiH}$ and ${}^7\text{LiD}$ as a function of the volume in the (NVT) ensemble, along QTB-MD runs about 6-7 ps as long, after equilibration.

For comparison purposes, we also performed QTB-MD simulations based on an empirical interionic potential. We adopted, for both ${}^7\text{LiH}$ and ${}^7\text{LiD}$, the same incompressible shell model developed by Haque and Islam [6] for ${}^7\text{LiH}$. This model allows to simulate electronic polarization in a phenomenological way. Periodic boundary conditions have been employed and the time step was equal to 5×10^{-16} s. For each simulation, the system of 1000 ions was equilibrated during 50 ps before the computation of average values, which were obtained along QTB-MD trajectories 50 ps as long.

We computed the density of states (DOS) of phonons by two distinct methods: (i) from MD runs through the Fourier transform of the velocity autocorrelation function [24] and (ii) from lattice dynamical properties within density functional perturbation theory (DFPT) by interpolating the interatomic force constants on a $40 \times 40 \times 40$ mesh in the Brillouin Zone. Concerning (i), the equilibrium configuration were generated in the (NVE) ensemble at a kinetic energy corresponding to that found within the QTB-MD simulation at 300 K. This temperature rescaling was used in order to recover the mean quantum vibrational energy [25]. For instance, at $T = 300$ K within the QTB, LiH shows a classical mean kinetic energy of 515 K. We chose to compute DOS along (NVE) trajectories, as, within QTB or Langevin dynamics, a spurious high-frequency tail would appear, because of the frictional coefficient γ .

3. Results and Discussion

3.1. Lattice parameter versus temperature

We choose the lattice parameter of ${}^7\text{LiD}$ at $T = 0$ K (hereafter noted a_0^{LiD}), as a reference value to define the isotopic shift. The experimental value (4.049 Å) [26] is reproduced within 1.2% by QTB-MD in the GGA (4.097 Å) and within 2.5% by QTB-MD employing the shell model [6] (4.152 Å). Our DFT value fairly compares with the QHA calculation in the GGA (4.077 Å) by Yu and coworkers [17]. We ascribe the tiny discrepancy with the latter value to the different pseudo-potentials used in the two calculations.

Here we focus on the isotopic shift in lattice parameter between ${}^7\text{LiH}$ and ${}^7\text{LiD}$, as a function of temperature T . The shifts are collected in figure 1. The experimental shifts are close to 0.016 and 0.014 Å at 0 K and 300 K, respectively. The isotopic shifts obtained from QTB-MD simulations within the GGA amount to 0.019 and 0.016 Å at 0 K and 300 K, respectively. QTB-MD simulations with the shell model yields 0.010 and 0.008 Å at 0 K and 300 K, slightly underestimating the experimental isotopic shift in the whole 0-300 K range.

As shown in figure 1, in both cases, the experimental trend in the isotopic shift is correctly reproduced by QTB-MD, although its precision depends on the representation of interatomic forces. We point out that the divergence between the lattice parameter that was computed neglecting quantum effects and that obtained by including them through the quantum thermal bath is much bigger than the isotopic shift itself. For instance, at 0 K, the inclusion of zero-point energy (ZPE) increases the ${}^7\text{LiD}$ lattice parameter by 0.069 Å when using the GGA and by 0.043 Å within the shell model.

3.2. Phonons

Isotope effects between vibrational spectra of ${}^7\text{LiH}$ and ${}^7\text{LiD}$ are mainly due to the difference in atomic masses. Indirect effects on interatomic forces due to the small difference in lattice constant can be safely neglected in the following discussion. figure 2 shows that vibrational DOS are similar in the acoustic part of the spectrum, at low frequencies, while optical contributions at higher frequencies differ substantially. This behavior fully agrees with Raman spectroscopy [27] and previous DFT calculations [13]. The shift in the optical region of the spectrum also involves larger zero-point effects for ${}^7\text{LiH}$ than ${}^7\text{LiD}$, which implies larger equilibrium volumes for the lighter isotope.

For instance, the experimental transverse optical frequency ν_{TO} , at ambient conditions, shifts from 17.7 THz (${}^7\text{LiH}$) down to 13.4 THz (${}^7\text{LiD}$) [28, 29]. In DFPT within the GGA, we chose ${}^7\text{LiH}$ and ${}^7\text{LiD}$ equilibrium volumes as determined by QTB-MD runs at zero pressure and $T = 300$ K, in order to compute the transversal optical frequencies. Both $\nu_{TO}({}^7\text{LiH}) = 15.5$ THz and $\nu_{TO}({}^7\text{LiD}) = 11.9$ THz were underestimated by about 10%, mainly as a consequence of the use of the GGA. The shell model severely underestimated these frequencies, $\nu_{TO}({}^7\text{LiH}) = 13.2$ THz and $\nu_{TO}({}^7\text{LiD}) = 10.0$ THz, which were computed through QTB-MD runs at constant

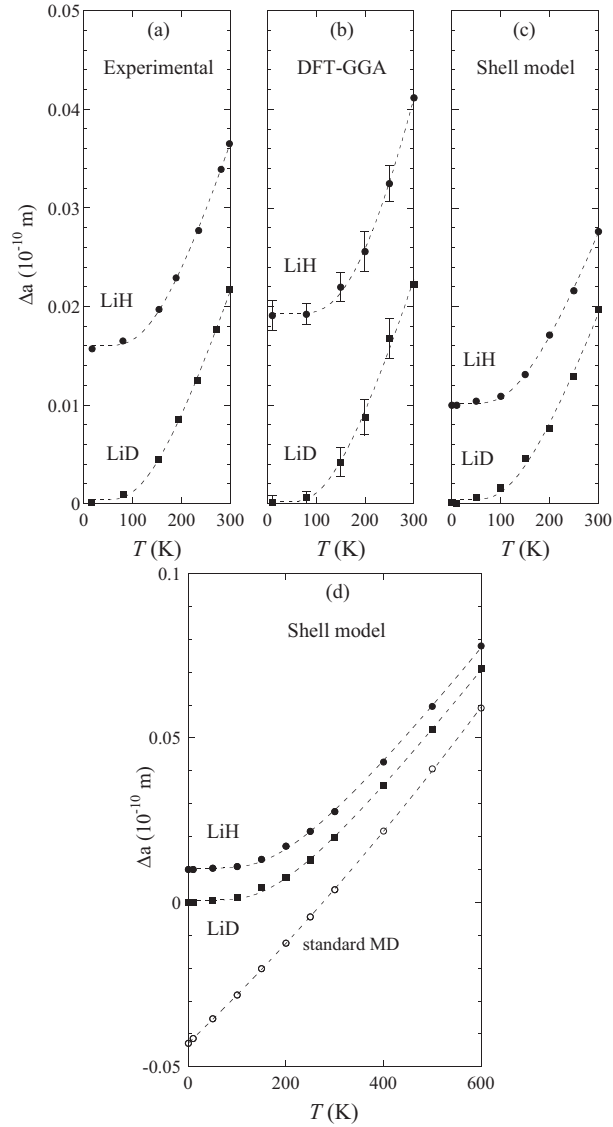


Figure 1. Isotopic shift in lattice parameter, $\Delta a = a - a_0^{LiD}$ for both ${}^7\text{LiH}$ and ${}^7\text{LiD}$, versus T . (a) Experimental results [26]; QTB-MD simulations by using (b) DFT within the GGA or (c) the shell model. Fits (dotted lines) were obtained through the expression $\Delta a = A + B/[\exp(T_D/T) - 1]$ where T_D is analogous to a Debye temperature. In order to point out quantum effects, panel (d) shows also the results of standard MD with the shell model up to $T = 600$ K, which leads to same results for ${}^7\text{LiH}$ and ${}^7\text{LiD}$.

volume. The ratio of transverse optical frequencies $\nu_{TO}(\text{LiH})/\nu_{TO}(\text{LiD})$ can be taken as a measure of the isotopic shift. Both experimental and simulated ratios give the expected inverse ratio between the square root of reduced masses, that is, $\sqrt{\mu({}^7\text{LiD})/\mu({}^7\text{LiH})} \simeq 1.3$.

Moreover, we found that anharmonic contributions to vibrations may be relevant. In order to estimate the importance of these contributions for thermal and mechanical properties of ${}^7\text{LiH}$ and ${}^7\text{LiD}$, we compared their phonon DOS, obtained through MD simulations in the (NVE) ensemble, as specified in Section 2, which correspond to

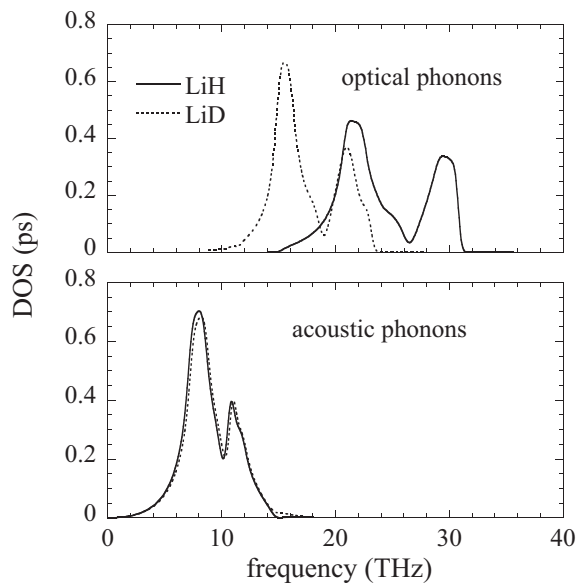


Figure 2. Vibrational DOS for ${}^7\text{LiH}$ and ${}^7\text{LiD}$ obtained through DFPT within the GGA for the optical and acoustic bands.

distinct mean kinetic energies. At $T = 1$ K, in particular, the system is in the harmonic regime.

Boronat *et al.* claimed that anharmonic effects are negligible at 20 K [30]; however, as shown in figure 3, we found that they are relevant in the vibrational spectra. For instance, for the lighter and more abundant ${}^7\text{LiH}$ isotope, the gap in the phonon DOS around $\nu \simeq 15$ THz in the harmonic regime was partially filled. Moreover, in the range of optical phonons, all peaks are smoothed; for $\nu \geq 32$ THz, phonons appear at frequency overtones, which were absent in the harmonic regime. Both characteristics are signatures of phonon-phonon interactions that are revealed by quantum effects, which cause LiH to probe the anharmonic part of the interatomic interactions. In the ${}^7\text{LiD}$ case, differences are less visible because of the smaller frequency range and the absence of the gap between acoustic and optical frequencies (figure 3).

3.3. Isotopic shift in pressure

The behavior of ${}^7\text{LiH}$ and ${}^7\text{LiD}$ at high pressures has been the object of considerable attention in past years. Experimental data were obtained by neutron [31] or x-ray diffraction [32]. The latter work showed that ${}^7\text{LiH}$ remains in a rocksalt structure up to 36 GPa and ${}^7\text{LiD}$ up to 94 GPa. Isotope effects on the equation of state (EOS) were discussed.

The EOS of ${}^7\text{LiH}$ and ${}^7\text{LiD}$ were fitted to *ab initio* QTB-MD data at $T=300$ K through the Vinet equation [21]. The resulting parameters, $a(P = 0)$, B and B' are listed and compared with experimental values in table 2. Therefore, within the statistical error, we did not find any isotopic shift in bulk modulus. This is consistent with the fact that acoustic phonons are pretty much the same in the two isotopes, as discussed

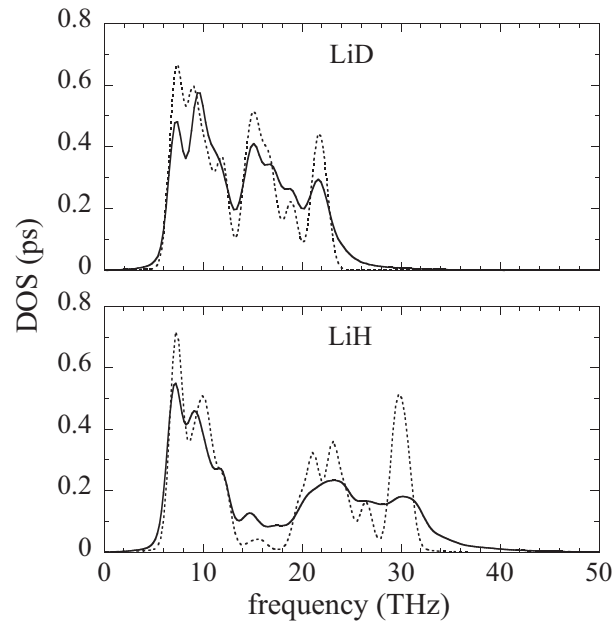


Figure 3. Vibrational DOS for ${}^7\text{LiH}$ and ${}^7\text{LiD}$. They have been computed via the Fourier transform of the velocity autocorrelation function within (NVE) MD, at 1 K (dashed line), or at 515 K (${}^7\text{LiH}$) and 435 K (${}^7\text{LiD}$) mean kinetic energies (full lines). In all simulations, the lattice parameter was set, for each isotope, to its ambient-temperature value including quantum effects, as shown in figure 1.

in the previous section. A similar behavior was reported [1] for other elastic constants, within the experimental uncertainty.

Table 2. Lattice parameter a , bulk modulus B , and its pressure derivative B' , for both ${}^7\text{LiD}$ and ${}^7\text{LiH}$ at $T = 300$ K and $P = 0$. All calculations adopted the GGA for the exchange-correlation energy functional.

| | MD-QTB this work | Exp. Ref.[32] | QHA Ref.[33] |
|-----------------------|---------------------|------------------|-----------------|
| $a(\text{LiD})$ (Å) | 4.116 | 4.070 | |
| $a(\text{LiH})$ (Å) | 4.135 | 4.081 | 4.142 |
| $B(\text{LiD})$ (GPa) | 29.2 ± 0.4 | 32.2 | |
| $B(\text{LiH})$ (GPa) | 28.6 ± 0.8 | 32.2 | 28.8 |
| $B'(\text{LiD})$ | 3.7 | 3.53 | |
| $B'(\text{LiH})$ | 3.7 | 3.53 | |

We computed the isotopic shift in pressure, ΔP , between ${}^7\text{LiH}$ and ${}^7\text{LiD}$ versus the applied pressure P on ${}^7\text{LiD}$ from QTB-MD simulations at 300K. Our results are close to the experimental data [32], in the whole 0-20 GPa range of applied pressures, both in value, in spite of being overestimated, and increasing trend (figure 4). Therefore, QTB-MD within the GGA reproduced the slope of isotopic shift in pressure accurately; in particular, the higher P , the smaller the volume, the more relevant quantum effects on nuclear motion become.

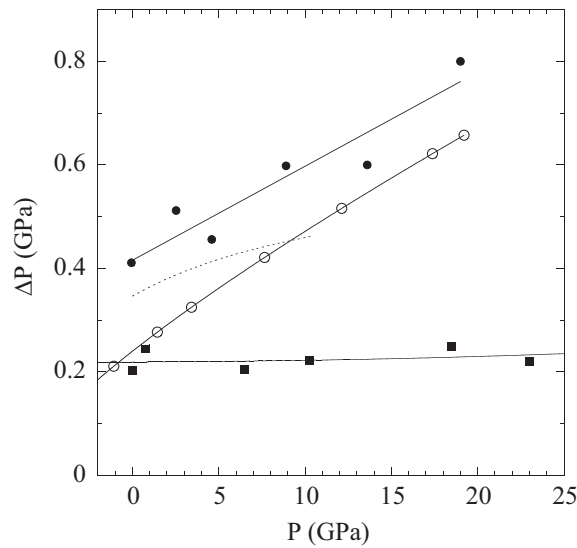


Figure 4. Isotopic shift, ΔP , defined as the difference in pressure between ${}^7\text{LiH}$ and ${}^7\text{LiD}$ at a given volume, versus pressure P in ${}^7\text{LiD}$. Filled circles and squares with a linear fit are QTBM-DFT-GGA and shell model, respectively. Open circles are experimental results [32] and dotted line is DFPT calculation of Ref. [13]. We mention that $\Delta P = 0$ in standard MD, whatever the atomic forces.

The pressure on lighter ${}^7\text{LiH}$ thus increases faster than on heavier ${}^7\text{LiD}$. QTBM-DFT-GGA simulations using the ${}^7\text{LiH}$ shell model of Haque and Islam [6] yielded constant ΔP (figure 4) close to the experimental value obtained for zero pressure on ${}^7\text{LiD}$. Therefore, this interatomic potential is not suitable to study lithium hydride at high pressures.

QHA within the DFPT [13] provided a fair estimate of the isotopic shift ΔP at low pressure on ${}^7\text{LiD}$ (figure 4). However, the slope of the curve ΔP significantly differed from the experimental one, especially at high pressures. Although the authors of ref. [13] used the LDA and different pseudopotentials from ours, we attribute this discrepancy to a failure of the quasi-harmonic approximation to represent the isotopic shift in pressure faithfully within the linear response regime. As pressure increases and volume shrinks, interatomic force constants get bigger and optical frequencies may substantially increase. Anharmonic contributions at high frequencies, which are not the same in ${}^7\text{LiH}$ and ${}^7\text{LiD}$, are not accounted for by the QHA (§3.2 and figure 3). We guess that this is the main reason why ΔP from the QHA diverges from experimental data at high pressure.

In order to discuss the behavior of isotopic shift in pressure ΔP at low P , we rely on the Murnaghan EOS [20]. From a Taylor expansion of the Murnaghan EOS in terms of the equilibrium volumes V_0 , bulk moduli B_0 and their pressure derivatives B'_0 for ${}^7\text{LiH}$ and ${}^7\text{LiD}$, respectively, one obtains:

$$\frac{\partial \Delta P}{\partial P} \simeq B'_0 \frac{\Delta V_0}{V_0} + \frac{\Delta B_0}{B_0} \quad (1)$$

where ΔV_0 and ΔB_0 are the isotopic shifts in equilibrium volume and bulk modulus, respectively; other quantities are referred to ${}^7\text{LiD}$. At $P \simeq 0$, experimental $\frac{\partial \Delta P}{\partial P} \simeq 2.5$; in our QTBM-DFT-GGA simulation within GGA, the first term (4.1) in equation (1) is much

bigger than the second one (-1.3), yielding $\frac{\partial \Delta P}{\partial P} \simeq 2.8$. Indeed, the isotopic shift in bulk modulus is almost null within DFT-GGA. QTB-MD simulations using the shell model provided a non negligible shift $\Delta B = -1$ GPa [36]. As a consequence, the two terms on the right side in equation (1) have opposite signs and almost compensate each other ($1.9, -2.2$), yielding a roughly constant ΔP , with null slope at the origin. Possibly, an improved shell model, fitted on high-pressure data, might reproduce the experimental isotopic shift in pressure.

4. Conclusion

We studied isotope effects in ${}^7\text{LiH}$ and ${}^7\text{LiD}$ by using a quantum thermal bath (QTB) that accounts for quantum effects on nuclear motion in molecular dynamics (MD) simulations. Two non-equivalent descriptions of interatomic forces have been considered: the *ab initio* DFT-GGA and a phenomenological approach using the shell model. In both cases, the experimental isotopic shift in the lattice parameter is reproduced, showing the adequacy of the QTB for describing such effects.

Acoustic vibrational DOS are similar for ${}^7\text{LiH}$ and ${}^7\text{LiD}$, while optical phonons are shifted to higher frequencies for ${}^7\text{LiH}$. The comparison of the phonon DOS obtained either in the harmonic regime or at kinetic energies that are representative of system dynamics including quantum effects illustrates the importance of anharmonic contributions.

QTB-MD within DFT-GGA reproduces the experimental isotopic shift in pressure with the correct slope, in contrast to the quasi-harmonic approximation, which fails at high pressures. The discrepancy between the two methods again demonstrates the importance of anharmonic contributions. Besides, QTB-MD by using the ${}^7\text{LiH}$ shell model of Haque *et al.* [6] does not provide the experimental slope of the isotopic shift in pressure. We attribute this discrepancy to the (likely erroneous) isotopic shift in bulk modulus as found within the shell model. Indeed, in both experiments and GGA-based QTB-MD simulations, bulk moduli of ${}^7\text{LiH}$ and ${}^7\text{LiD}$ are equal within the statistical uncertainty whereas, for the shell model, the isotopic shift in bulk modulus is significant. These results might provide a route to derive suitable shell models for reliable simulations of light elements at high pressures. A new potential could be obtained by fitting the shell-model parameters to the Vinet equation of state derived from static DFT-GGA calculations without any quantum effects. Its validity could be checked by taking into account isotopic shifts in bulk modulus and pressure.

References

- [1] Plekhanov V G 2003 *Physics Uspekhi* **46** 689
- [2] Atzeni S and Meyer-Ter-Vehn J 2004 *The physics of inertial fusion* (Oxford: Oxford Science Publications)
- [3] Grochala W and Edwards P P 2004 *Chem. Rev.* **104** 1283
- [4] Cazorla C and Boronat J 2005 *J. Low Temp. Phys.* **139** 645

- [5] Allen R E and de Wette F W 1969 *Phys. Rev.* **179** 873
- [6] Haque E and Islam A K M A 1990 *Phys. Stat. Sol. (b)* **158** 457
- [7] Marx D, Tuckerman M E, Hutter J and Parrinello M *Nature (London)* **397** 601
- [8] Dammak H, Chalopin Y, Laroche M, Hayoun M and Greffet J J 2009 *Phys. Rev. Lett.* **103** 190601
- [9] Ceriotti M, Bussi G and Parrinello M 2009 *Phys. Rev. Lett.* **103** 030603
- [10] Dammak H, Hayoun M, Chalopin Y and Greffet J J 2011 *Phys. Rev. Lett.* **107** 198902
- [11] Ceriotti M, Manolopoulos D E and Parrinello M 2011 *J. Chem. Phys.* **134** 084104
- [12] Perdew J P, Burke K and Ernzerhof M 1996 *Phys. Rev. Lett.* **77** 3865
- [13] Roma G, Bertoni C M and Baroni S 1996 *Solid State Commun.* **98** 203
- [14] Troullier N and J. L. Martins J L 1991 *Phys. Rev. B* **43** 1993
- [15] Fuchs M and Scheffler M 1999 *Comput. Phys. Commun.* **119** 67
- [16] Lebègue S, Alouani M, Arnaud B and Pickett W E 2003 *Europhys. Lett.* **63** 562
- [17] Yu W, Jin C, and Kohlmeyer A 2007 *J. Phys.: Condens. Matter* **19** 086209
- [18] Gonze X *et al.* 2009 *Computer Phys. Commun.* **180** 2582
- [19] Bottin F, Leroux S, Knyazev A and Zerah G 2008 *Comput. Mat. Science* **42** 329
- [20] Murnaghan F D 1937 *Am. J. Math.* **49** 235
- [21] Vinet P, Ferrante J, Smith J R and Rose J H 1986 *J. Phys. C* **19** L467
- [22] Martyna G J, Tuckerman M E, Tobias D J and Klein M L 1996 *Mol. Phys.* **87** 1117
- [23] Barrat J L and Rodney D 2011 *J. Stat. Phys.* **144** 679
- [24] Dickey J M and Paskin A 1969 *Phys. Rev.* **188** 1407
- [25] Wang C Z, Shan C T and Ho K M 1990 *Phys. Rev. B* **42** 11276
- [26] Smith D K and Leider H R 1968 *J. Appl. Cryst.* **1** 246
- [27] Ho A C, Hanson R C and Chizmeshya A 1997 *Phys. Rev. B* **55** 14818
- [28] Verble J L, Warren J L and Yarnell J L 1968 *Phys. Rev.* **168** 980
- [29] Laplace D 1977 *J. Phys. C: Solid State Phys.* **10** 3499
- [30] Boronat J, Cazorla C, Colognesi D and Zoppi M 2004 *Phys. Rev. B* **69** 174302
- [31] Besson J M, Weill G, Hamel G, Nelmes R J and Loveday J S 1992 *Phys. Rev. B* **45** 2613
- [32] Loubeyre P, Le Toullec R, Hanfland M, Ulivi L, Datchi F and Hausermann D 1998 *Phys. Rev. B* **57** 10403
- [33] Barrera G D, Colognesi D, Mitchell P C H and Ramirez-Cuesta A J 2005 *Chem. Phys.* **317** 119
- [34] Mukherjee D, Sahoo B D, Joshi K D, Gupta S C and Sikka S K 2011 *J. Appl. Phys.* **109** 103515
- [35] Birch F 1947 *Phys. Rev. B* **71** 809
- [36] At $T = 300\text{K}$, fitted B_0 are 44.5 GPa and 45.5 GPa for ${}^7\text{LiH}$ and ${}^7\text{LiD}$, respectively, when using the shell model.